Position sensitive detection of neutrons in high radiation background field

Article *in* The Review of scientific instruments · February 2014

DOI: 10.1063/1.4862478 · Source: PubMed

4 authors:

Daniel Vavrik
Institute of Theoretical and Applied Mechanics of the CAS
131 PUBLICATIONS **1,180** CITATIONS
SEE PROFILE

Jan Jakubek
Advacam s.r.o.
583 PUBLICATIONS **32,428** CITATIONS
SEE PROFILE

Stanislav Pospisil
Czech Technical University in Prague
1,186 PUBLICATIONS **56,499** CITATIONS
SEE PROFILE

Jiri Vacik
Nuclear Physics Institute of the CAS v.v.i.
305 PUBLICATIONS **2,765** CITATIONS
SEE PROFILE

Position sensitive detection of neutrons in high radiation background field

D. Vavrik, J. Jakubek, S. Pospisil, and J. Vacik

Citation: Review of Scientific Instruments **85**, 013304 (2014); doi: 10.1063/1.4862478
View online: http://dx.doi.org/10.1063/1.4862478
View Table of Contents: http://scitation.aip.org/content/aip/journal/rsi/85/1?ver=pdfcov
Published by the AIP Publishing

Position sensitive detection of neutrons in high radiation background field

D. Vavrik,[1,2,a)] J. Jakubek,[2] S. Pospisil,[2] and J. Vacik[3]
[1]*Institute of Experimental and Applied Physics, Czech Technical University in Prague, Horska 3a/22, Prague, Czech Republic*
[2]*Institute of Theoretical and Applied Mechanics, Academy of Sciences of the Czech Republic, Prosecka 76, 190 00 Prague 9, Czech Republic*
[3]*Nuclear Physics Institute, Academy of Sciences of the Czech Republic, Rez, 250 68 Prague, Czech Republic*

(Received 4 November 2013; accepted 6 January 2014; published online 27 January 2014)

We present the development of a high-resolution position sensitive device for detection of slow neutrons in the environment of extremely high γ and e^- radiation background. We make use of a planar silicon pixelated (pixel size: 55 × 55 μm^2) spectroscopic Timepix detector adapted for neutron detection utilizing very thin ^{10}B converter placed onto detector surface. We demonstrate that electromagnetic radiation background can be discriminated from the neutron signal utilizing the fact that each particle type produces characteristic ionization tracks in the pixelated detector. Particular tracks can be distinguished by their 2D shape (in the detector plane) and spectroscopic response using single event analysis. A Cd sheet served as thermal neutron stopper as well as intensive source of gamma rays and energetic electrons. Highly efficient discrimination was successful even at very low neutron to electromagnetic background ratio about 10^{-4}. © *2014 AIP Publishing LLC*.
[http://dx.doi.org/10.1063/1.4862478]

INTRODUCTION

This paper aims to utilizing a silicon pixelated detector covered by thin ^{10}B conversion layer for position sensitive detection of slow neutrons with enhanced signal-to-background ratio. Especial attention is devoted to the discrimination of the signal comprised by γ and e^- radiation from the pursued neutron signal in the situation of extremely high ratio (10^4) between background (γ and e^-) and neutron signal.

The reliable position sensitive detection of slow neutrons in extremely high γ radiation background accompanied by electrons utilizing a semiconductor detector covered with converter generating heavy charged particles[1,2] (such as ^6Li or ^{10}B) is limited by the ability to separate the neutron signal from the background. The passive and/or active approach can be used for this separation. As passive approach we can list several possibilities. The shielding of the neutron detector by high Z material is not too effective as the γ background is suppressed partially only and additional e^- background is generated by this shielding.[3] The γ background can be suppressed reducing the thickness of the active volume of the semiconductor sensor.[2,4] The high-energy threshold setting represents another simple and effective solution of this problem if the detector has this capability,[5] which can reduce both the e^- and γ background signal. However, both approaches have some limitation under extremely high background conditions as will be demonstrated in this paper.

Regardless all above-mentioned techniques can be used the active and highly efficient solution is to utilize single event–spectroscopic analysis of traces of the detected particles in the pixel detector (analogy of "event discrimination according event shape and energy"). We make use of the energy sensitive pixelated semiconductor Timepix[6] device for this purpose, which was originally designed for single event X-ray photon detection. The conversion of thermal neutrons into detectable radiation is realized using appropriate converter, such as ^{10}B. This reaction exhibits high cross sections of 3837 barns for (n, α) reactions with two channels:

$$^{10}B + n \begin{matrix} \rightarrow \alpha_1^*(1.47MeV) + {}^7Li^*(0.84meV) + \gamma \\ \rightarrow \alpha_0(1.78MeV) + {}^7Li(1.01MeV) \end{matrix} . \quad (1)$$

Note that first channel of this nuclear reaction has probability 93.7 %. The converter in the form of a thin layer is placed onto the detector surface. The reaction products as well as γ rays and electrons interacting in the detector sensitive volume create e-h charge pairs. This charge is collected by the pixels of the detector, which are arranged into a planar orthogonal matrix in the Timepix detector used. Heavy charged particles α and ^7Li are used for position sensitive detection of neutrons, while the signals caused by γ from background and neutron induced nuclear reactions have to be suppressed. The particle type recognition is an essential task for this reason.

In the Timepix detector, each ionizing particle type forms a characteristic track pattern with characteristic energy profile, which corresponds to the path of the particle in sensitive volume and its ionizing power. Besides of the particle type, for given detector parameters (sensor material/thickness and bias voltage), the track characteristics depend also on the particle energy and flight direction. The track pattern is formed as a cluster of pixels with measurable signal. This pattern can be described by its 2D geometry projected onto the detector plane, where the signal value is not evaluated (i.e., only the existence of a measurable signal for each pixel is recorded). Basic particle type recognition is based on the track pattern analysis. The energy profile of the track is given by the evaluation of the signal in the track pixels. The sum of energies collected by all track pixels gives information about the energy deposited by a single particle. The spectroscopic information obtained in this way allows more accurate identification of

a)Author to whom correspondence should be addressed. Electronic mail: vavrik@itam.cas.cz.

the particle type using spectral peaks corresponding to known nuclear reactions.

It will be shown that discrimination of heavy charged particles (HCP) from γ, which is based on track pattern characteristics only, is not sufficient enough for suppression of extremely high radiation background as presented in this paper. However, spectroscopic analysis of each track enables practically full suppression of this background. Moreover, HCP types (α or ^{7}Li in our case) are reliable differentiated using spectroscopic analysis. The converter thickness can be optimized from the point of view of the detection efficiency, particle recognition correctness, and accuracy of position sensitive detection. Spectroscopic properties of the "detector–converter arrangement" and the spatial resolution of position sensitive detection improve with decreasing converter thickness.[10,11] A very thin converter was chosen since particle recognition is fundamental for this work apart from the low detection efficiency.

INSTRUMENTATION

Neutron source

A thermal neutron beam from the LWR-15 research reactor[7] of the Nuclear Physics Institute, Academy of Sciences of the Czech Republic and the Research Centre Rez was used. This beam is primarily designed for the neutron depth profiling technique.[8] The thermal neutron beam has an intensity of 3×10^6 neutrons/s cm^2 with Maxwellian energy distribution at the reactor power of 6 MW and has a quite high purity – prevalently thermal neutrons are present in this beam (Cd ratio is $\sim 10^5$) with relatively low intensity of γ rays. The geometrical cross section of the beam at the exit of the neutron guide is 80 mm (width) $\times$ 4 mm (height).

Timepix detector

We employed a Timepix detector chip equipped with a 300 μm thick silicon sensor with total active area of 14×14 mm^2. The silicon sensor is bump bonded to 256 $\times$ 256 matrix of square pixels with 55 μm pitch. Timepix is controlled and read out using the USB 2.0 based interface FITpix.[16] Each individual Timepix pixel can work in one of three modes: Counting mode, where the number of registered events is counted; Time of Arrival, for which the particle detection time is measured in relation with time of exposure; and Time over Threshold mode (TOT), which measures the time when the pulse produced in spectroscopic chain of individual pixel is above a preselected threshold[6] and permits measurement of the deposited charge. The TOT mode is used in this work.

The charge measured by the individual detector pixels in TOT mode is transformed into the energy scale using a per-pixel energy calibration.[9] The Timepix detector was calibrated in the range 6–60 keV using several fluorescent and radioactive gamma ray sources. The obtained charge-energy dependence was linearly extrapolated to the MeV energy range.

Converter layer

A very thin converter layer was prepared in order to register and separate signals of both heavy charged products α, ^{7}Li from the nuclear reaction (1). For this purpose, the sputtering technique was used for depositing ^{10}B onto a thin (1.5 μm) Biaxially Oriented Polypropylene Terephthalate (BoPET) foil. The technique of Neutron Depth Profiling (NDP) 8 was used to measure the layer thickness. The thickness of the compact ^{10}B converter was determined to be 1.8 μg/cm^2 ($\sim$36 nm). It has been shown that up to 1 μm thick layer still has good spectroscopic properties.[10]

Generation of extremely high gamma and e$^-$ background

A 0.6 mm thick Cd sheet with a wedge window served as a neutron absorber and as a generator of extremely high gamma and e$^-$ background to show the ability to detect heavy charged particles in highly unfavourable conditions.

The Cd sheet and BoPET foil with the ^{10}B layer were attached onto the sensor surface by ^{10}B converter side, using a thin cover glass (thickness 0.15 mm, Borosilicate with 8.4% of B_2O_3) and a metal clasp (see Fig. 1). These components were stacked in the following order: sensor, converter, foil, glass and clasp. The effective amount of 10B in the cover glass was 0.04 mg/cm^2 (the range of HCP in glass is $\sim$4 mm), which is almost 50 times smaller than the thickness of the converter on the BoPET foil. HCP produced by the cover glass are moreover attenuated by the BoPET foil. It was found using simulation[12] that energy of all ^{7}Li particles passed through BoPET foil decreasing bellow 0.4 MeV. The attenuation of the thermal neutrons by the cover glass was evaluated as 0.012%.

Single event analysis

The separation of the radiation background signal from the neutron signal was done using the so-called single event analysis,[11] performed by custom made plugin of the Pixelman software.[12] The single event analysis evaluates track shape (cluster of active pixels) and/or its energy profile of each recorded particle (event). For illustration, how different particle types can be distinguished[11] see Fig. 2: tracks of X-ray photons or low energy γ rays have shape of small dots (a);

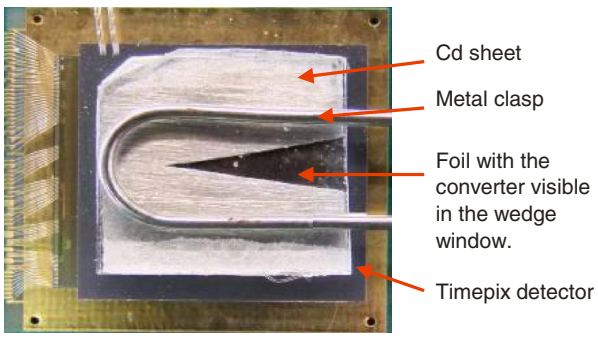

FIG. 1. Timepix detector adapted for the position sensitive neutron detection. Cd sheet serving as neutron absorber and γ generator laying between cover grass and foil with converter. Wedge window is cut in the Cd sheet.

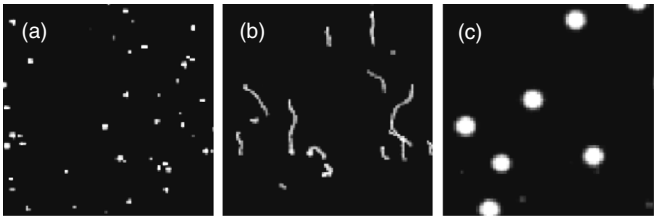

FIG. 2. Characteristic tracks for different particle types as imaged by the Timepix detector: 60 keV photons (a), high energy 0.546 MeV electrons (b), and 5.5 MeV alpha particles (c).

high energy e^- have typically long tracks (b); clusters corresponding to HCP (c).

The visualized track form is determined by the particle path "itself'' and is influenced also by charge diffusion in the semiconductor sensor. Note that high-energy γ rays generate high energy e^- electrons in the silicon sensor. HCPs typically produce circular shape tracks with Gaussian distribution[13] of the energy (charge) deposited in the sensor. Although it is usually easy to distinguish a HCP track from an e^- track, e^- tracks can be occasionally also circular (spiral) and similar to the HCP track.

An example of a HCP track recorded by the energy sensitive pixel detector Timepix is depicted in Fig. 3.

The charge distribution of this track has the form of a discrete Gaussian since the charge diffuses in the sensor and is shared across the discrete pixel matrix of the detector. The 2D track pattern (the projection of the track shape onto the detector plane) tends to be circular (for short range HCP). The diameter of this circle is given by the particle energy, the bias voltage applied on the sensor electrode, the sensor material/thickness, and the detection threshold of individual pixels (around 3 keV for the Timepix used). The maximum of the measured charge (energy) lies in the track center.

The typical signal of a HCP can be imaged as a discrete 3D bar plot (each bar represents the energy deposited in each detector pixel) and can be fitted by a 2D Gaussian convoluted with the pixel response function[14] (Gaussian fit) is depicted in Fig. 4.

Differences between e^- and HCP tracks visible in Fig. 2 can be qualified using "evident" pattern recognition criteria, which are summarized in Table I. Strongest pattern recognition criteria for HCP discrimination are: "*Area*" – number of

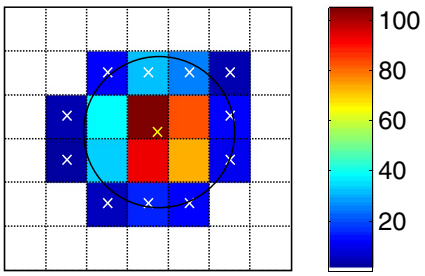

FIG. 3. Discrete Gaussian track imaged by Timepix. The color represents the energy deposited in each pixel. The border pixels are labeled by white crosses. This track has parameters (Tables I and II): *Area* = 17, *Maximum distance from the circle* = 0.51, *Roundness* = 0.78, *Cluster volume* = 0.59 MeV, *Registered amplitude* = 103 keV.

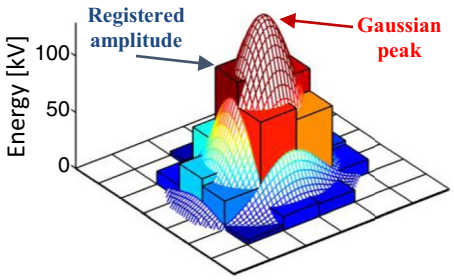

FIG. 4. Discrete Gaussian imaged as 3D bar plot fitted by smooth 2D function (Gaussian convoluted with the detector pixel response function).

pixels in one track in relation with the particle energy; "*Maximal distance from the circle*" – difference from ideally circular track which decreases for increasing discrete Gaussian area; "*Roundness*" – higher value indicates the elongation (protrusion) of the track; "*Continuous interior area*" – indicates whether the track has not a gap inside. Note, that pattern recognition criteria can be applied also for a detector without spectroscopic ability.

It will be shown below that these pattern recognition criteria are not strong enough to discriminate all e^- from HCP. Therefore, additional energetic criteria are introduced; thanks to the use of a detector with per-pixel energy measurement capability. The charge measured by the Timepix detector used is transformed into the energy scale. The energetic criteria with highest impact for HCP identification are listed in Table II: "*Minimal registered amplitude*" – minimal value of the track energy peak in conjunction with the pattern area ensures that particle can be classified as heavy; "*Cluster volume*" – measuring of the energy deposited in one track, it allows distinguishing between different particle types using their known spectral properties; "*Maximum in the center only*" – is used for elimination of the track with local minimum inside; "*Normalized chi-square test*" – characterizes the probability that the cluster has Gaussian profile.

RESULTS

The Timepix device was placed on the neutron beam. For the measurement a total of 3.03×10^5 frames were acquired

TABLE I. Overview of the evident pattern recognition criteria used for particle discrimination.

Pattern criterion	Value
Continuous interior area	Yes/No: inner pixels of the track pattern form/not form continuous area.
Area	Number of pixels in the track: 1 for one pixel event; tens for energetic e^- and heavy charged particles.
Roundness	Evaluated as the ratio between the closest and the most distant boundary pixels from the center of gravity of the track. It is ~1 for ideally circular track.
Maximal distance from the circle	Measured as the difference between the track boundary pixels and a circle, which has identical area as analyzed track. It is ~0 for an ideally circular track.

TABLE II. Overview of the energetic and cluster shape criteria used for particle identification.

Energetic criterion	Value
Maximum in the center only	Yes if the cluster has single local energy maximum located in the track center, i.e., the cluster is not affected by pileup or it is not an electron with circular/spiral track.
Minimal registered amplitude	The energy peak of the track has to be higher than specific value of this parameter for a particle with energy equal or higher than searched.
Normalized chi-square test	~1: calculated from deviations of the cluster energy profile from Gaussian fit, normalized by the track area. This test utilizes the fact that even compact (circular/spiral) e^- track has not a Gaussian distribution.
Cluster volume	The sum of energies deposited in all pixels of the track analyzed – spectroscopic information.

using the USB 2 readout interface FITpix.[15] The high-count rate required short exposure time down to 5 ms to minimalize pileup of individual tracks in one exposed frame.

An example of a frame acquired by Timepix detector in TOT mode is shown in Fig. 5. The prevalent number of tracks corresponds to unwanted electrons and gammas from neutron capture in Cd. These particles mainly produce curved line tracks. Only one α particle was detected in this frame.

The window wedge presence is evident in Fig. 6, where all frames were summed without any data processing (total 5.4×10^7 events were registered). The neutron beam intensity profile with a 4 mm height is clearly pronounced in the image.

Searching of the optimal parameters for single event analysis

First of all the evident pattern recognition criteria were optimized to reject energetic electrons with long track and electrons with point like track. We started the analysis with relatively lightly affecting values of pattern recognition criteria. These criteria were gradually set stringent. Optimization was reached when number of clusters corresponding to HCP started dramatically to decrease. Optimized criteria are listed in Table III. The influence of a given parameter on particle

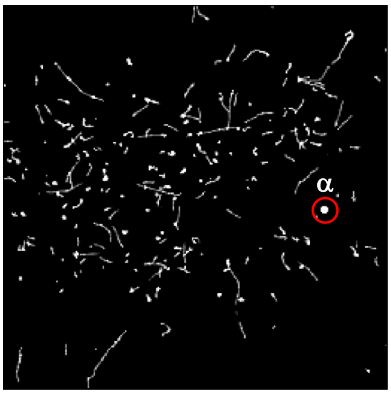

FIG. 5. The example of a frame acquired (the image size is 14 × 14 mm, 256 × 256 pixels). The alpha particle identified is marked by the red circle. All others events are e^- tracks.

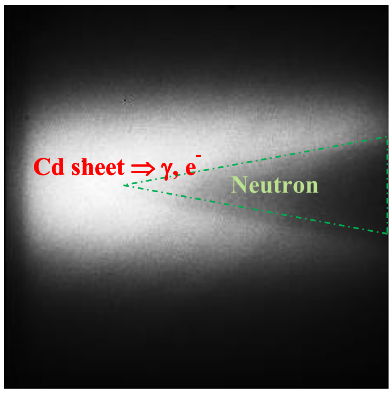

FIG. 6. Sum of all frames without particle discrimination. The neutron beam is oriented horizontally. The strongest signal arises from electrons and gammas generated in the Cd sheet.

identification for heavy charged particles is expressed by the value called *Impact* (the fraction of events evaluated as background). Totally 96.7% of all tracks were classified as non-heavy charged particles using the pattern recognition criteria only.

The image in Fig. 7(a) represents the sum of the first 5 $\times 10^3$ frames for which single event analysis has been done using optimized pattern recognition criteria. One can see that some electrons are still falsely identified as HCP as shown in the region, where Cd covers part of the detector, see the magnified region Fig. 7(b). The probability that a HCP track appears in this region is very low because of very low neutron flux at this area. The main source of falsely identified particles using pattern recognition criteria only is the fact that sometimes e^- tracks can exhibit a circular (spiral) shape, with a pattern similar to HCP pattern. However, such falsely identified tracks can be rejected utilizing the energetic criteria. Our investigation of the effective energetic criteria is based on the spectra analysis as described below.

Two separated rectangular regions of interest (ROI) in the area of the wedge window (^{10}B ROI, only ^{10}B converter is presented in this ROI) and of the area with the Cd sheet covering ^{10}B converter (Cd ROI), see Fig. 8, were selected.

Detailed spectroscopic analysis of the signal was processed in these ROIs. The ROI spectra are displayed in Fig. 9.

The signal of gammas and electrons prevails in both ROIs spectra, namely, only the pattern recognition procedure is applied to discriminate the gamma and electrons, see curves in blue and blue dotted, respectively. The effective application of pattern recognition criteria on discrimination of gammas and electrons signal from HCP is clear on the signal from

TABLE III. Values of optimized pattern recognition criteria.

Criterion	Value	Impact
Continuous interior area	Yes	16%
Area	≥16	68.6%
Roundness	≥0.75	11.4%
Maximum distance from the circle	≤0.5	0.7%

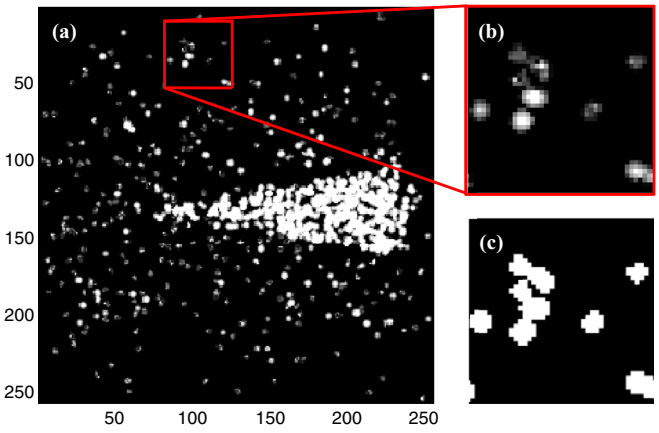

FIG. 7. Sum of events identified as HCP using pattern recognition criteria integrated over 5 × 103 frames (a). Magnified detail of the region overlaid by the Cd sheet (b). Tracks in this area are produced by electrons. However, without energy information the tracks look similar to HCP tracks (c).

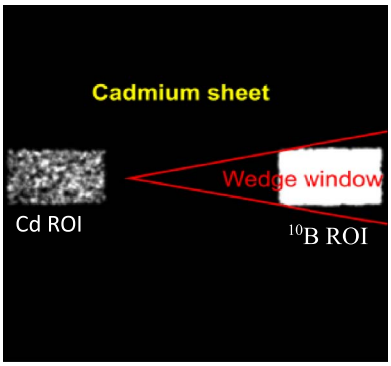

FIG. 8. Signal in Cd ROI (left) and in ^{10}B ROI (right). Edges of the wedge window are highlighted in red.

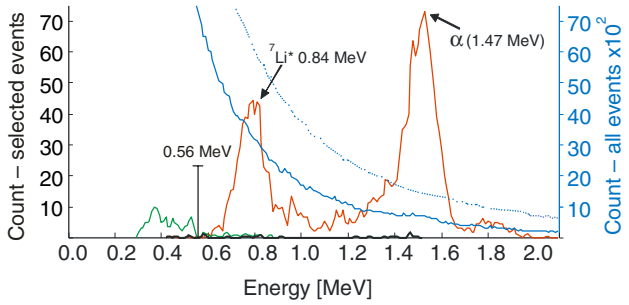

FIG. 9. Blue curve: full ^{10}B ROI spectrum of all events; blue dotted: Cd ROI spectrum of all events (scale right). Green curve: Cd ROI – pattern recognition criteria only (see Cd ROI in Fig. 8). Red curve: ^{10}B ROI – all criteria used for events selection (scale left). Black curve: Cd ROI – all criteria applied.

TABLE IV. Values of optimized energetic and cluster shape criteria.

Criterion	Value	Impact
Maximum in the center only	True	3.4%
Lower limit of registered peak	≥94	43.5%
Normalized chi-square test	≤1.1	14.9%
^{7}Li and α separation	Value	Fraction
Energy in cluster (MeV): ^{7}Li	<1.1	33%
Energy in cluster (MeV): α	>1.1	77%

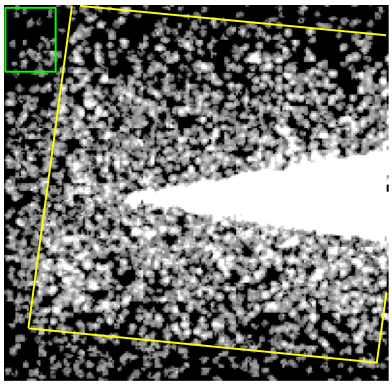

FIG. 10. Neutron imaging using the pattern recognition criteria. The converter edges are plotted in yellow.

Cd ROI spectrum (no HCP are expected there), where the signal is quite well suppressed with the exception of small contribution in the low energy part, see graph in green.

The energetic and cluster shape criteria given in Table II were then applied on the events already preselected using pattern recognition criteria (3.3% of all events remained only). We found that for the effective discrimination of electrons from the HCP events (^{7}Li and α), the *Minimal registered amplitude* has to be higher than 96 keV.[17] Concurrently all ^{7}Li particles from the cover glass are discriminated by this criteria and resultant HCP signal from cover glass is 100x lower than from the converter. The energetic criteria *Maximum in the center only* and *Chi-square test* were applied as well. Optimized values of these energetic criteria are summarized in the first column of Table IV. Actual values of their impact for heavy particle discrimination depend on the order of the criteria applied.

By applying of energetic and cluster shape criteria, the electron signal in Cd ROI was finally completely suppressed; see black curve plot in Fig. 9. The weak HCP signal, which remains in Cd ROI signal, corresponds to epithermal or scattered neutrons reaching the converter. Contrary to the ^{10}B ROI spectrum, where even though all criteria were applied the ^{10}B and α signal remains strong and clear, see red curve in Fig. 9. Peaks related to nuclear reaction (1) are nicely resolved, and the e^- and γ signal are completely discriminated there. The ^{7}Li and α_1 peaks are well separated by the energy distance of 0.63 MeV as it should be. The fraction of ^{7}Li identified was less than two times lower than fraction of α, see second column in Table IV. The main reason for the lower count of ^{7}Li than α is due to larger self-absorption of the emitted ^{7}Li nuclei in the ^{10}B converter and the insensitive ohmic contact layer on the sensor.[10]

Analyzing of the whole data set

Finally the whole data set from the ^{10}B experiment was processed by analyzing all tracks. HCP interacting in the detector and identified using pattern recognition criteria only are imaged in Fig. 10, and using all criteria (listed in Tables III and IV) are imaged in Fig. 11. The negligible signal should be registered in the green box top left, behind the Cd sheet

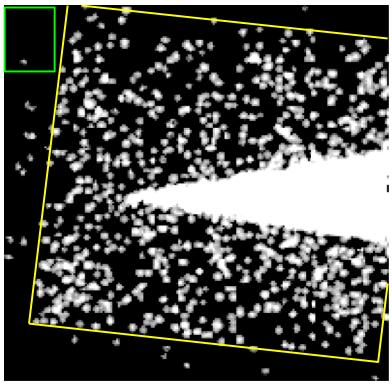

FIG. 11. Imaging using both pattern recognition and energetic criteria. Almost no signal is outside the converter area.

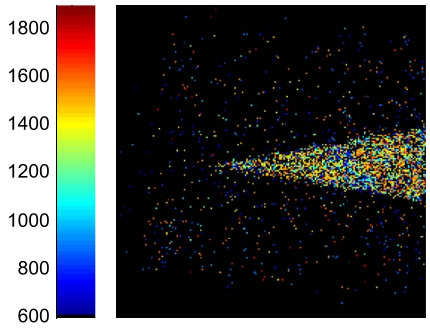

FIG. 13. Registration of ^{7}Li events (plotted in shades of blue: 0.6–1.1 MeV) and α particles (green to red: 1.1–2.1 MeV, keV scale).

outside of the neutron beam center, where the converter is not present. Despite this, 29 particles identified as HCP using pattern recognition criteria only were detected in this box, see Fig. 10, top left.

On the contrary, only one particle was identified as HCP in the green box using all criteria (probably spiral e^- track); see Fig. 11. It is evident that the background was successfully suppressed. Finally about 5.3×10^3 alpha and ^{7}Li particles from 5.4×10^7 events were identified in the whole data set using all criteria. Hence, one can conclude that the proposed technique works well even for a signal to background ratio of $\sim 10^{-4}$.

Spectra from the whole data set (whole detector area) were calculated similarly as in the section before. The spectrum of all events, without any particle discrimination, is plotted in blue in Fig. 12. Background events dominate in this spectrum. The spectrum of all HCP is plotted in red in Fig. 12. Peaks corresponding to the ^{7}Li* and α* particles are well separated. It is even possible to see a signal in the areas where peaks corresponding to ^{7}Li and α particles are expected.

The distribution of positions[16] of these HCP with detector pixel resolution (55 μm) is displayed in Fig. 13. Note that the value of the particle counts fluctuates over the wedge window. It is caused by statistical fluctuations and thickness inhomogeneity of the ^{10}B converter itself, and probably also due to nonhomogeneous thickness of the insensitive layer on the sensor surface.

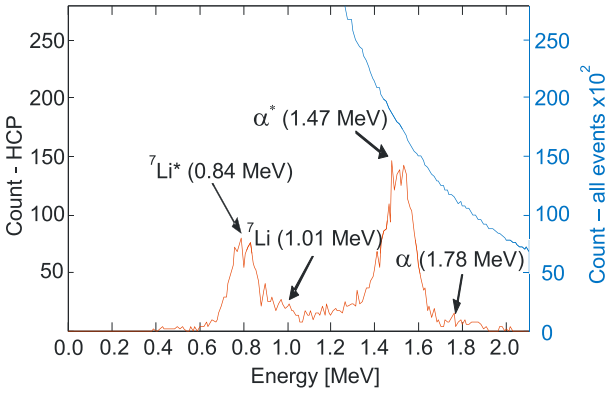

FIG. 12. Spectrum of all events without any discrimination of γ and e^- (blue curve top right). Spectrum of all events after discrimination of the γ and e^- background (red curve), where well resolved peaks of ^{7}Li and α are well enhanced even at rather low statistic.

CONCLUSIONS

We have evaluated the criteria to be used for effective discrimination of signal induced by gammas and electrons in silicon sensor of the pixel detector Timepix to be used for high-resolution position sensitive detection of neutrons. The criteria have been applied in the so-called "tracking" mode when the clusters produced by individually interacting quanta of radiation in the silicon pixel sensor are individually analyzed:

- Pattern recognition criteria used for heavy particle discrimination leads to no negligible amount of false identified heavy charged particles, since a significant amount of electrons may have a similar track pattern as heavy charged particles.
- Energetic and cluster shape criteria employing spectral analysis of the analyzed particles significantly improve neutron signal discrimination.

The actual impact of each criterion for particle identification depends on the sequence of its application. Pattern recognition criteria have lower computation cost than energetic criteria and therefore these are applied first.

It has been shown that the proposed methodology based on single event analysis of particle tracks in semiconductor pixel detectors can be effectively used for position sensitive neutron detection even in environments with extremely high gamma ray and electron background radiation. It has been proven that it works even at a signal to background ratio of about 10^{-4}. The ability to determine the position of individual neutrons is not perturbed at all.

ACKNOWLEDGMENTS

This research is carried out in the frame of the CERN Medipix Collaboration, and has been supported by the projects TA01010237 of the Technology Agency of the Czech Republic; P108/12/G108 of the Grant Agency of the Czech

Republic; CZ.1.05/1.1.00/02.0060 of the European Regional Development Fund and Ministry of Education Youth and Sports of the Czech Republic.

[1]S. Pospíšil, B. Sopko, E. Havránková, Z. Janout, J. Koníček, I. Mácha, and J. Pavlů, "Si diode as a small detector of slow neutrons," Radiat. Protect. Dos. **46**, 115 (1993); available at http://rpd.oxfordjournals.org/content/46/2/115.abstract.

[2]D. S. McGregor, D. S. J. T. Lindsay, C. C. Brannon, and R. W. Olsen, "Semi-insulating bulk GaAs thermal neutron imaging arrays," IEEE Trans. Nucl. Sci. **43**, 1357 (1996).

[3]Y. K. Haga, S. Kumazawa, and N. Niimura, "Gamma-ray sensitivity and shielding of a neutron imaging plate," J. Appl. Cryst. **32**, 878 (1999).

[4]J. Hůlka, Z. Kánský, Z. Janout, and S. Pospíšil, "Thermal neutron detector utilizing semiconductor silicon detector with surface barrier (Detektor tepelných neutronů využívající křemíkový polovodičový detektor s povrchovou bariérou)," Acta Polytechnica **8**(IV. 1), 93–104 (1980).

[5]J. Jakubek, T. Holy, E. Lehmann, S. Pospisil, J. Uher, J. Vacik, and D. Vavrik, "Neutron imaging with Medipix-2 chip and a coated sensor," Nucl. Instrum. Meth. A **560**, 143 (2006).

[6]X. Llopart, R. Ballabriga, M. Campbell, L. Tlustos, and W. Wong, "Timepix, a 65k programmable pixel readout chip for arrival time, energy and/or photon counting measurements," Nucl. Instrum. Meth. A **581**, 485 (2007).

[7]Nuclear Physics Institute AS CR & Research Centre Rez, Reactor LVR-15; see home page: http://www.cvrez.cz/web/en/reactor-lvr-15.

[8]J. Vacik, J. Cervena, V. Hnatowicz, V. Havranek, J. Hoffmann, S. Poxta, D. Fink, and R. Klett, "Pulse-shape discrimination in neutron depth profiling technique," Nucl. Instrum. Meth. B **142**, 397 (1998).

[9]J. Jakubek, "Precise energy calibration of pixel detector working in time-over-threshold mode," Nucl. Instrum. Meth. A **633**, S262 (2011).

[10]M. Voytchev, M. P. Iñiguez, R. Méndez, A. Mañanes, L. R. Rodríguez, and R. Barquero, "Neutron detection with a silicon PIN photodiode and 6LiF converter," Nucl. Instrum. Meth. A **512**, 546 (2003).

[11]T. Holy, E. Hayne, J. Jakubek, S. Pospisil, J. Uher, and Z. Vykydal, "Pattern recognition of tracks induced by individual quanta of ionizing radiation in Medipix2 silicon detector," Nucl. Instrum. Meth. A **591**, 287 (2008).

[12]J. Ziegler, M. Ziegler, and J. Biersack, "SRIM - The Stopping and range of Ions in matter," Nucl. Instrum. Meth. in Physics Research B **268**, 1818 (2010), software homepage: www.srim.org.

[13]J. Jakubek, A. Cejnarova, T. Holy, S. Pospisil, J. Uher, and Z. Vykydal, "Pixel detectors for imaging with heavy charged particles," Nucl. Instrum. Meth. A **591**, 155 (2008).

[14]F. Krejčí, J. Jakůbek, M. Kroupa, V. Jurka, and K. Hruška, "Semiconductor pixel detector with absorption grid as a tool for charge sharing studies and energy resolution improvement," J. Instrum. **6**, C12034 (2011).

[15]V. Kraus, M. Holik, J. Jakubek, P. Soukup, and Z. Vykydal, "FITPix - fast interface for Timepix pixel detectors," J. Instrum. **6**, C01079 (2011).

[16]J. Jakubek, P. Schmidt-Wellenburg, P. Geltenbort, M. Platkevic, C. Plonka-Spehr, J. Solc, and T. Soldner, "A coated pixel device Timepix with micron spatial resolution for UCN detection," Nucl. Instrum. Meth. A **600**, 651 (2009).

[17]This value comes from the assumption that the track *Area* has to be $\geq$16 (square 4 $\times$ 4 for instance) and *Cluster volume* $\geq$0.56 MeV (local drop down minimum in the Cd ROI spectra after pattern recognition criteria application – green line in Fig. 9).